

On the generic increase of entropy in isolated systems

Zhiqiang Huang¹ and Qing-yu Cai^{2,3,*}

¹*State Key Laboratory of Magnetic Resonance and Atomic and Molecular Physics,
Innovation Academy for Precision Measurement Science and Technology,
Chinese Academy of Sciences, Wuhan 430071, China*

²*Center for Theoretical Physics, Hainan University, Haikou 570228, China*

³*School of Information and Communication Engineering, Hainan University, Haikou 570228, China*

(Dated: June 11, 2025)

This study establishes a universal mechanism for entropy production in isolated quantum systems governed by the eigenstate thermalization hypothesis (ETH). By developing a resolvent-based framework, we demonstrate that steady-state entropy generically arises from many-body interactions, independent of specific coupling details. Analytical arguments reveal that entropy generation is driven by two universal pathways: interaction-induced energy broadening and temporal coarse-graining over exponentially small energy gaps. Numerical simulations of nonintegrable Ising spin chains confirm logarithmic entropy scaling, consistent with predictions derived from ETH-governed eigenstate mixing. The derived self-consistent equations for energy shift and broadening parameters agree closely with numerical results. These results unify observational entropy concepts with von Neumann entropy dynamics, providing predictive tools for thermodynamic behavior in quantum many-body systems. Our findings resolve longstanding debates about interaction-dependent entropy scaling and offer pathways for entropy control in quantum technologies.

I. INTRODUCTION

The thermalization of isolated quantum systems remains a fundamental puzzle at the intersection of quantum mechanics and statistical physics. While classical systems achieve equilibrium through microscopic chaos and ergodicity, the unitary evolution of quantum systems imposes strict constraints on entropy production—a contradiction resolved only through modern frameworks such as the ETH [1–4]. Over the past decade, significant progress has been made in understanding how quantum many-body systems reconcile deterministic dynamics with emergent statistical behavior. However, a critical gap persists: while ETH explains local thermalization, the origin and universality of entropy growth in the full system require deeper elucidation, especially under weak coupling and finite-size conditions.

Recent theoretical advances have identified observational entropy, a measure quantifying information loss from coarse-grained measurements, as a key framework bridging quantum dynamics and thermodynamics [5–7]. A parallel line of research has focused on the role of temporal coarse-graining, averaging observables over long timescales, in mimicking thermodynamic irreversibility. This approach, formalized in the steady-state hypothesis [8–10], posits that time-averaged states of closed systems exhibit thermal properties despite unitary constraints. These developments underscore the need to unify disparate entropy-generation mechanisms, such as quantum entanglement, energy redistribution, and measurement-induced decoherence, into a coherent predictive framework.

While these frameworks have significantly advanced thermodynamic descriptions, their ability to elucidate the microscopic mechanisms of entropy production remains limited due to several factors. First, the relationship between interaction strength and entropy production is still inadequately characterized, particularly in systems near the threshold of integrability. Second, the universality of entropy growth, whether it is governed solely by global properties such as the density of states or requires finely tuned interactions, remains an open question. Moreover, the emergence of deep thermalization [11, 12] (higher-order correlations matching random state statistics) has expanded the scope of thermalization criteria, demanding refined entropy measures.

In this work, we address these challenges by establishing a universal mechanism for entropy production in ETH-obeying systems, independent of specific interaction details. Building on recent advances in resolvent-based methods and energy-shell averaging, we demonstrate that steady-state entropy arises generically from eigenstate mixing governed by the system’s intrinsic non-integrability. Our approach circumvents restrictive assumptions of earlier models, such as random matrix interactions, by leveraging ETH’s universal predictions for matrix element statistics. Through a combination of analytical arguments and large-scale numerical simulations of nonintegrable spin chains, we identify two dominant entropy-generation pathways: (1) interaction-induced delocalization [4] of quantum information across the energy spectrum, and (2) temporal averaging over exponentially small energy gaps.

This study bridges critical gaps between abstract thermalization theory and practical entropy quantification. By demonstrating that generic systems exhibit logarithmic entropy scaling with interaction bandwidth, a direct consequence of Lorentzian energy broadening, we provide

* qycal@hainanu.edu.cn

a predictive framework for thermodynamic behavior in quantum many-body systems. Our results offering tools to optimize entropy control in quantum technologies. The universal features identified here not only deepen our understanding of quantum statistical mechanics but also provide the foundation for designing nonequilibrium states with tailored entropy dynamics.

II. STEADY STATE OF A CLOSED SYSTEM

Consider a system S and a bath B that are initially independent, with the unperturbed Hamiltonian $H_0 = H_S + H_B$. Assume their initial states are energy eigenstates $|\phi_{\mu i}\rangle = |\phi_i^S\rangle \otimes |\phi_{\mu}^B\rangle$, satisfying $H_0 |\phi_{\mu i}\rangle = a_{\mu i} |\phi_{\mu i}\rangle$, where $a_{\mu i} = E_i + \epsilon_{\mu}$. When an interaction V is introduced, the total Hamiltonian becomes $H = H_0 + V$, with eigenstates $|\psi_n\rangle$ obeying $H |\psi_n\rangle = \lambda_n |\psi_n\rangle$.

We analyze the time evolution of the initially uncorrelated state $|\phi_{\mu i}\rangle$ under the interacting Hamiltonian H . In this scenario, entanglement and correlations develop between the system and bath. The corresponding density matrix is $\rho(t) = U(t) |\phi_{\mu i}\rangle \langle \phi_{\mu i}| U^\dagger(t)$. Under long-time evolution (i.e., over timescales exceeding the decoherence time), the composite system-bath approaches a steady state defined by:

$$\omega := \lim_{t \rightarrow \infty} \frac{1}{t} \int_0^t \rho(\tau) d\tau. \quad (1)$$

For non-degenerate systems, this steady state corresponds to the decohered state in the energy eigenbasis:

$$\omega = \sum_n \Pi_n \rho(0) \Pi_n = \sum_n \Pi_n |\langle \psi_n | \phi_{\mu i} \rangle|^2, \quad (2)$$

where $\Pi_n = |\psi_n\rangle \langle \psi_n|$. Letting $|\langle \psi_n | \phi_{\mu i} \rangle|^2 = p_n^{\mu i}$, the Shannon entropy of the decohered state becomes:

$$S(\omega) = - \sum_n p_n^{\mu i} \ln p_n^{\mu i}. \quad (3)$$

As a special case, when no interaction is introduced ($V = 0$), the density matrix remains in a pure state $\omega = |\phi_{\mu i}\rangle \langle \phi_{\mu i}|$. In this scenario, its entropy remains zero with no entropy production.

Since the composite system is initially in a pure state (zero entropy), the steady-state entropy $S(\omega)$ quantifies the entropy production in the closed system. This entropy generation originates from two mechanisms: (1) interaction-induced system-bath entanglement, and (2) the temporal coarse-graining inherent in long-time observations. In this work, we focus on analyzing the steady-state entropy production.

III. STEADY-STATE ENTROPY INCREASE

We first analyze the general properties of the probability distribution $p_n^{\mu i}$ in coherent states. Using random

interactions modeled by Hermitian band matrices V with Gaussian-distributed entries, previous work [13] demonstrated that the expected distribution of $p_n^{\mu i}$ follows a Cauchy-Lorentz form:

$$p_n^{\mu i} \approx \frac{1}{\pi} \frac{\gamma_i}{(a_{\mu i} - \lambda_n - \eta_i)^2 + \gamma_i^2}. \quad (4)$$

In this work, we consider general interactions while assuming validity of the ETH. For ETH-satisfying systems, as the particle number N increases: (1) The energy range scales linearly with N , (2) The Hilbert space dimension (number of eigenstates) grows exponentially, (3) Energy gaps decrease exponentially.

From a perturbation perspective, exponentially small gaps at large N violate the smallness condition $|V_{\mu i, \nu j} / (a_{\mu i} - a_{\nu j})| \ll 1$, making the problem non-perturbative. Letting $Z = zI$ (where I denotes the identity matrix) and employing the resolvent identity:

$$\frac{1}{Z - H} = \frac{1}{Z - H_0} + \frac{1}{Z - H_0} V \frac{1}{Z - H}, \quad (5)$$

we derive:

$$\begin{aligned} & \left(1 - \frac{1}{z - a_{\mu i}} V_{\mu i, \mu i}\right) \langle \phi_{\mu i} | \frac{1}{Z - H} | \phi_{\mu i} \rangle \\ &= \frac{1}{z - a_{\mu i}} + \frac{1}{z - a_{\mu i}} \langle \phi_{\mu i} | V \Phi_{\mu i} \frac{1}{Z - H} | \phi_{\mu i} \rangle, \end{aligned} \quad (6)$$

where the interaction matrix elements are defined as $V_{\mu i, \nu j} = \langle \phi_{\mu i} | V | \phi_{\nu j} \rangle$, and the projection operator $\Phi_{\mu i} = I - |\phi_{\mu i}\rangle \langle \phi_{\mu i}|$ excludes the self-interaction contribution from the basis state. Applying (5) further yields:

$$\begin{aligned} \Phi_{\mu i} \frac{1}{Z - H} | \phi_{\mu i} \rangle &= \frac{\Phi_{\mu i}}{Z - H_0} V \Phi_{\mu i} \frac{1}{Z - H} | \phi_{\mu i} \rangle \\ &+ \frac{\Phi_{\mu i}}{Z - H_0} V | \phi_{\mu i} \rangle \langle \phi_{\mu i} | \frac{1}{Z - H} | \phi_{\mu i} \rangle, \end{aligned} \quad (7)$$

leading to the self-consistent equation:

$$\begin{aligned} & \left(I - \frac{\Phi_{\mu i}}{Z - H_0} V \Phi_{\mu i}\right) \Phi_{\mu i} \frac{1}{Z - H} | \phi_{\mu i} \rangle \\ &= \frac{\Phi_{\mu i}}{Z - H_0} V | \phi_{\mu i} \rangle \langle \phi_{\mu i} | \frac{1}{Z - H} | \phi_{\mu i} \rangle. \end{aligned} \quad (8)$$

Substituting into (6) produces the closed resolvent equation:

$$\mathcal{R}_{\mu i}(z) = \frac{1}{z - a_{\mu i} - V_{\mu i} - \mathcal{G}_{\mu i}}, \quad (9)$$

where the projected resolvent $\mathcal{R}_{\mu i}(z) := \langle \phi_{\mu i} | \frac{1}{Z - H} | \phi_{\mu i} \rangle$, $V_{\mu i} = \langle \phi_{\mu i} | V | \phi_{\mu i} \rangle$, and

$$\begin{aligned} \mathcal{G}_{\mu i} &= \langle \phi_{\mu i} | V \left(\Phi_{\mu i} - \frac{\Phi_{\mu i}}{Z - H_0} V \Phi_{\mu i} \right)^{-1} \frac{\Phi_{\mu i}}{Z - H_0} V | \phi_{\mu i} \rangle \\ &= \langle \phi_{\mu i} | V \Phi_{\mu i} \frac{1}{Z - H} \Phi_{\mu i} V | \phi_{\mu i} \rangle. \end{aligned} \quad (10)$$

The term $\mathcal{G}_{\mu i}$ decomposes into two distinct contributions:
1. Off-diagonal elements:

$$\sum_{\nu j \neq \mu i} |V_{\mu i, \nu j}|^2 \langle \phi_{\nu j} | \frac{1}{Z-H} | \phi_{\nu j} \rangle, \quad (11)$$

2. The cross-correlated terms:

$$\sum_{\nu j \neq \xi k \neq \mu i} V_{\mu i, \nu j} V_{\xi k, \mu i} \langle \phi_{\nu j} | \frac{1}{Z-H} | \phi_{\xi k} \rangle. \quad (12)$$

The interaction can be decomposed as $V = \sum_{ij} \Pi_{ij}^S \otimes O_{ij}^{B_1}$, where B_1 represents a small subsystem within the bath B . For quantum systems obeying ETH, the matrix elements of local operators in the energy eigenbasis follow the universal relation [4]:

$$|\langle \phi_\mu | O^{B_1} | \phi_\nu \rangle|^2 = e^{-S(\epsilon_{\mu\nu}^+)} f^2(\epsilon_{\mu\nu}^+, \delta) |R_{\mu\nu}|^2, \quad \mu \neq \nu, \quad (13)$$

where $\epsilon_{\mu\nu}^+ = (\epsilon_\mu + \epsilon_\nu)/2$, $\delta = \epsilon_\mu - \epsilon_\nu$, $e^{S(\epsilon)}$ denotes the bath's density of states, $f(\epsilon, \delta)$ are smooth functions, and $R_{\mu\nu}$ characterizes random matrix fluctuations with Hermitian symmetry.

Considering the exponential scaling of state numbers with N , statistical treatment of summations over indices μ, ν, ξ reduces to evaluating their ensemble averages. For cross-correlated ETH terms:

$$(O^{B_1})_{\mu\nu} (O^{B_1})_{\xi\mu} \propto R_{\mu\nu} R_{\xi\mu}, \quad \mu \neq \nu \neq \xi, \quad (14)$$

the statistical independence of $R_{\mu\nu}$ leads to [14]:

$$\mathbb{E}(R_{\mu\nu} R_{\xi\mu}) = 0, \quad \mu \neq \nu \neq \xi. \quad (15)$$

When considering single-term interactions $V = O^S \otimes O^{B_1}$, combining (15) with (10) eliminates cross-correlations, producing:

$$\mathcal{G}_{\mu i}(z) = \sum_{\nu j \neq \mu i} |V_{\mu i, \nu j}|^2 \mathcal{R}_{\nu j}(z). \quad (16)$$

For more complex multi-term interactions, additional analysis of statistical relationships between random variables under different observables becomes necessary:

$$\mathbb{E}(R_{\mu\nu}^{ij} R_{\xi\mu}^{ki}), \quad \mu i \neq \nu j \neq \xi k, \quad (17)$$

where R^{ij} corresponds to the ETH random variables associated with local observables $O_{ij}^{B_1}$. The vanishing property of ensemble average eq. (17) depends on specific interaction forms, which currently lacks systematic investigation and requires further development. Given that ETH manifests as an intrinsic local property of energy eigenstates independent of specific observable operator, we postulate:

$$\mathbb{E}(R_{\mu\nu}^{ij} R_{\xi\mu}^{ki}) = 0, \quad \mu \neq \nu \neq \xi. \quad (18)$$

This leads to a crucial distinction from the cross-correlated ETH terms addressed in eq. (16). Whereas

those terms become negligible, we must now consider their contributions through:

$$\begin{aligned} \mathcal{G}_{\mu i}(z) &= \sum_{\nu j \neq \mu i} |V_{\mu i, \nu j}|^2 \mathcal{R}_{\nu j}(z) \\ &+ \sum_{\nu j \neq \mu i; k \neq j} V_{\mu i, \nu j} V_{\nu k, \mu i} \mathcal{R}_{\nu j}^k(z), \end{aligned} \quad (19)$$

where the cross-contribution term is defined as

$$\mathcal{R}_{\nu j}^k(z) = \langle \phi_{\nu j} | \frac{1}{Z-H} | \phi_{\nu k} \rangle \quad (20)$$

Through eq. (5) and utilizing $\mathbb{E}(R_{\mu\nu}) = 0$ for $\mu \neq \nu$, we derive the recursive expression

$$\mathcal{R}_{\nu j}^k(z) = \sum_l \frac{1}{z - a_{\nu j}} V_{\nu j, \nu l} \mathcal{R}_{\nu l}^k(z). \quad (21)$$

The inclusion of $\mathcal{R}_{\nu j}^k(z)$ significantly increases the complexity of self-consistent equations. To maintain analytical tractability and focus on fundamental mechanisms, this work intentionally restricts its scope to regimes where cross-correlated terms remain negligible.

Substituting (16) into (9) establishes a self-consistent equation for $\mathcal{R}_{\mu i}(z)$. To connect this to the probability distribution $p_n^{\mu i}$, we exploit the completeness relation of perturbed eigenstates:

$$\mathcal{R}_{\mu i}(z) = \sum_n \frac{p_n^{\mu i}}{z - \lambda_n}. \quad (22)$$

Using the Sokhotski-Plemelj identity:

$$\frac{1}{x - i0^+} = \mathcal{P} \left(\frac{1}{x} \right) + i\pi \delta(x), \quad (23)$$

the imaginary component of $\mathcal{R}_{\mu i}$ maps to the spectral measure:

$$\frac{1}{\pi} \text{Im} \mathcal{R}_{\mu i}(x - i0^+) = \sum_n p_n^{\mu i} \delta(x - \lambda_n). \quad (24)$$

This defines $p_n^{\mu i}$ via energy binning:

$$\begin{aligned} p_n^{\mu i} &= \int_{(\lambda_{n-1} + \lambda_n)/2}^{(\lambda_n + \lambda_{n+1})/2} dx \frac{1}{\pi} \text{Im} \mathcal{R}_{\mu i}(x - i0^+) \\ &= \frac{1}{e^{S(\lambda_n)}} \frac{1}{\pi} \text{Im} \mathcal{R}_{\mu i}(x - i0^+). \end{aligned} \quad (25)$$

The analytic continuation $H \rightarrow H + i0^+$ shifts $\mathcal{R}_{\mu i}(x) \rightarrow \mathcal{R}_{\mu i}(x - i0^+)$. From (9),

$$\mathcal{R}_{\mu i}(x - i0^+) = \frac{1}{x - a_{\mu i} - V_{\mu i} - \mathcal{G}_{\mu i}(x - i0^+)}. \quad (26)$$

Combining with (25), the probability distribution becomes:

$$p_n^{\mu i} = \frac{1}{\pi e^{S(\lambda_n)}} \frac{\text{Im} \mathcal{G}_{\mu i}(\lambda_n - i0^+)}{[\Delta_n^{\mu i} - \text{Re} \mathcal{G}_{\mu i}(\lambda_n)]^2 + [\text{Im} \mathcal{G}_{\mu i}(\lambda_n - i0^+)]^2}, \quad (27)$$

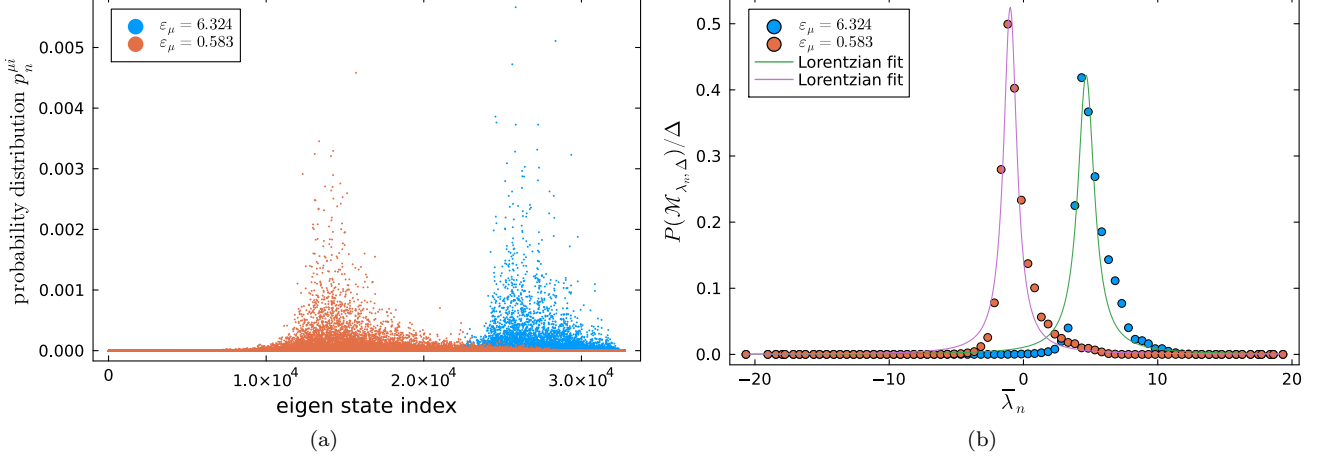


FIG. 1. (a) Probability distribution $p_n^{\mu i}$ ($i = 1$) versus eigenstate index n (sorted by energy) for the composite system. (b) Binned distribution $P(\mathcal{M}_{\lambda, \Delta})$ constructed by summing probabilities within energy intervals $\mathcal{M}_{\lambda, \Delta}$, where $\Delta = 0.5$, following Eq. (33). The binned probability is expressed as $P(\mathcal{M}_{\lambda, \Delta}) = \int_{\lambda - \Delta/2}^{\lambda + \Delta/2} d\lambda_m e^{S(\lambda_m)} p^{\mu i}(\lambda_m)$, with $\bar{\lambda}_n$ representing the average eigenenergy within each interval. Solid curves show Lorentzian fits to the binned distributions. Fitting parameters: For $\epsilon_\mu = 6.324$, we obtain $a_{\mu i} + \Delta_{\mu i} = 4.661$ and $\chi_{\mu i} = 0.753$; for $\epsilon_\mu = 0.583$, the parameters are $a_{\mu i} + \Delta_{\mu i} = -0.986$ and $\chi_{\mu i} = 0.606$.

where $\Delta_{\mu i} = \lambda_n - a_{\mu i} - V_{\mu i}$. By (16) and (24):

$$\begin{aligned} \frac{1}{\pi} \text{Im} \mathcal{G}_{\mu i}(\lambda_n - i0^+) &= \sum_{\nu j \neq \mu i} |V_{\mu i, \nu j}|^2 \sum_m p_m^{\nu j} \delta(\lambda_n - \lambda_m) \\ &= \sum_{\nu j \neq \mu i} |V_{\mu i, \nu j}|^2 e^{S(\lambda_n)} p_n^{\nu j}, \end{aligned} \quad (28)$$

in which we used the continuum approximation $\sum_m \rightarrow \int d\lambda e^{S(\lambda)}$. The real part of $\mathcal{G}_{\mu i}$ derives from the principal value integral:

$$\oint dx \frac{1}{\pi} \text{Im} \mathcal{R}_{\mu i}(x - i0^+) \frac{1}{z - x} = \sum_n \frac{p_n^{\mu i}}{z - \lambda_n} = \mathcal{R}_{\mu i}(z). \quad (29)$$

Thus,

$$\begin{aligned} \text{Re} \mathcal{G}_{\mu i}(\lambda_n) &= \oint dx \frac{1}{\pi} \text{Im} \mathcal{G}_{\mu i}(x - i0^+) \frac{1}{\lambda_n - x} \\ &= \sum_{\nu j \neq \mu i} |V_{\mu i, \nu j}|^2 \oint d\lambda_m \frac{1}{\lambda_n - \lambda_m} e^{S(\lambda_m)} p_m^{\nu j} \\ &= \sum_{\nu j \neq \mu i} |V_{\mu i, \nu j}|^2 \sum_{m \neq n} \frac{p_m^{\nu j}}{\lambda_n - \lambda_m}. \end{aligned} \quad (30)$$

Substituting (30) and (28) into (27) yields a closed self-consistent equation for $p_n^{\mu i}$. This formalism enables iterative solutions: (1) Initialization: Assume a trial distribution $p_n^{\mu i}$. (2) Update: Compute $\mathcal{G}_{\mu i}$ via (28) and (30). (3) Convergence: Reconstruct $p_n^{\mu i}$ through (27). Rapid convergence arises because nonintegrable systems inherently favor quasi-Lorentzian distributions, conforming to the self-consistent equation's structure.

An alternative pathway to determine the statistical behavior of $p_n^{\mu i}$ involves solving self-consistent equations using an ansatz. Given the inherent stochasticity of $p_n^{\mu i}$, we focus on statistical averaging within energy shells. Partitioning eigenstates into energy intervals:

$$\mathcal{M}_{E, \Delta} = (E - \Delta/2, E + \Delta/2), \quad (31)$$

the smoothed probability distribution becomes:

$$p^{\mu i}(\lambda) = \mathbb{E}(p_n^{\mu i}) := \frac{1}{d_{\mathcal{M}}} \sum_{\lambda_m \in \mathcal{M}_{\lambda, \Delta}} p_m^{\mu i}, \quad (32)$$

where $d_{\mathcal{M}} = e^{S(\lambda)} \Delta$ denotes the Hilbert space dimension within the shell. Guided by equation (27) and supported by numerical evidence, we adopt the minimal Lorentzian ansatz formulation:

$$\begin{aligned} p^{\mu i}(\lambda) &= \frac{1}{e^{S(\lambda)}} \frac{1}{\pi} \text{Im} \left(\frac{1}{\lambda - a_{\mu i} - \Delta_{\mu i} - i\chi_{\mu i}} \right) \\ &= \frac{1}{e^{S(\lambda)}} \frac{1}{\pi} \frac{\chi_{\mu i}}{(\lambda - a_{\mu i} - \Delta_{\mu i})^2 + \chi_{\mu i}^2}. \end{aligned} \quad (33)$$

This form inherently satisfies normalization due to Lorentzian properties:

$$\sum_n p_n^{\mu i} = \int d\lambda \frac{1}{\pi} \frac{\chi_{\mu i}}{(\lambda - a_{\mu i} - \Delta_{\mu i})^2 + \chi_{\mu i}^2} = 1. \quad (34)$$

The ansatz reduces the self-consistent equations for $p_n^{\mu i}$ to determining parameters $\chi_{\mu i}$ (width) and $\Delta_{\mu i}$ (shift). It should be noted that the distribution (33) is only a smooth distribution about λ in a statistical sense. It only represents the statistical behavior of $p_n^{\mu i}$. Therefore, the

self-consistent equations corresponding to the parameters $\chi_{\mu i}$ and $\Delta_{\mu i}$ are also only valid in a statistical sense.

The self-consistent equation form of the parameters $\chi_{\mu i}$ and $\Delta_{\mu i}$ is still very complicated. Here we make the most direct separation: By comparing eqs. (27) and (33), for different μi , after taking the appropriate λ , we should have

$$\begin{aligned}\chi_{\mu i} &= \mathbb{E}(\text{Im } \mathcal{G}_{\mu i}(\lambda - i0^+)), \\ \Delta_{\mu i} &= V_{\mu i} + \mathbb{E}(\text{Re } \mathcal{G}_{\mu i}(\lambda)).\end{aligned}\quad (35)$$

Substituting (28), (30) and (33) produces explicit equations:

$$\begin{aligned}\chi_{\mu i} &= \sum_{\nu j \neq \mu i} |V_{\mu i, \nu j}|^2 \frac{\chi_{\nu j}}{(\lambda - a_{\nu j} - \Delta_{\nu j})^2 + \chi_{\nu j}^2}, \\ \Delta_{\mu i} - V_{\mu i} &= \sum_{\nu j \neq \mu i} |V_{\mu i, \nu j}|^2 \frac{\lambda - a_{\nu j} - \Delta_{\nu j}}{(\lambda - a_{\nu j} - \Delta_{\nu j})^2 + \chi_{\nu j}^2}.\end{aligned}\quad (36)$$

$$(37)$$

These coupled equations enable iterative determination of $\chi_{\mu i}$ and $\Delta_{\mu i}$ for specific interaction profiles $|V_{\mu i, \nu j}|^2$.

The entropy of the smoothed distribution (33) evaluates to:

$$\begin{aligned}S(p^{\mu i}) &= - \int d\lambda e^{S(\lambda)} p^{\mu i}(\lambda) \ln p^{\mu i}(\lambda) \\ &= \int d\lambda \frac{S(\lambda)}{\pi} \frac{\chi_{\mu i}}{(\lambda - a_{\mu i} - \Delta_{\mu i})^2 + \chi_{\mu i}^2} + \ln(4\pi\chi_{\mu i}) \\ &\approx S(a_{\mu i} + \Delta_{\mu i}) + \ln(4\pi\chi_{\mu i}),\end{aligned}\quad (38)$$

where the first term reflects the density of states at the shifted energy, and the second term quantifies the width of the Lorentzian distribution. The entropy derived in eq. (38) demonstrates close correspondence with observational entropy [7], as both approaches employ a smoothing procedure that approximates the state distribution within the energy shell as a maximally mixed state. This smoothing scheme results in an overestimated entropy compared to the true entropy of the probability distribution $p_n^{\mu i}$, since actual entropy reduction arises from probability fluctuations within the energy shell.

IV. NUMERICAL RESULTS

To validate our theoretical framework, we conduct numerical simulations on an Ising spin chain with both transverse and longitudinal magnetic fields. The system Hamiltonian is given by:

$$H = \sum_{k=1}^N (-\sigma_z^k \otimes \sigma_z^{k+1} + g\sigma_x^k + h\sigma_z^k), \quad (39)$$

where $g = 1.05$ and $h = 0.1$ in our implementation. This system exhibits nonintegrability except when either

g or h vanishes. While periodic boundary conditions are adopted for simplicity, our conclusions remain valid for arbitrary boundary conditions. We construct the composite system with $N = 15$ spins:

- System S : Single spin governed by $H_S = g\sigma_x^S + h\sigma_z^S$
- Bath B : Remaining 14 spins following $H_E = -\sum_{k=1}^{13} \sigma_z^k \otimes \sigma_z^{k+1} + \sum_{k=1}^{14} (g\sigma_x^k + h\sigma_z^k)$
- System-bath interaction: $V = -\sigma_z^S \otimes (\sigma_z^1 + \sigma_z^{14})$

The system energies approximately satisfy $E_i \approx (-1)^i 1.055$, distinguishing two energy branches.

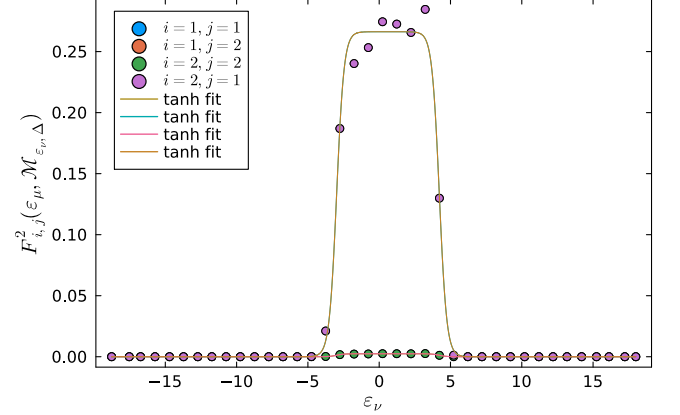


FIG. 2. Interaction strength distribution analysis. We calculate $F_{i,j}^2(\epsilon_\mu, \mathcal{M}_{\epsilon_\nu, \Delta}) := \sum_{\epsilon_\kappa \in \mathcal{M}_{\epsilon_\nu, \Delta}} |V_{\mu i, \kappa j}|^2 = \int_{\epsilon_\nu - \Delta/2}^{\epsilon_\nu + \Delta/2} d\epsilon_\kappa f_{i,j}^2(\epsilon_\mu, \delta)$ with $\epsilon_\mu = 0.583$ and $\Delta = 1.0$. The horizontal axis denotes ϵ_ν . Fitting results yield: $F_{1,1}^2 = F_{2,2}^2 = 0.001 \times \{\tanh[1.930(x + 2.985)] + \tanh[1.930(4.216 - x)]\}$ and $F_{1,2}^2 = F_{2,1}^2 = 0.133 \times \{\tanh[1.930(x + 2.985)] + \tanh[1.930(4.216 - x)]\}$, demonstrating distinct coupling channels.

We perform numerical simulations using this nonintegrable model. By directly diagonalizing the Hamiltonians H_0 and H , we obtain their respective energy eigenstates. The transition probability distribution $p_n^{\mu i}$ is calculated through eigenstate inner products $|\langle \psi_n | \phi_{\mu i} \rangle|^2$. This distribution is subsequently smoothed by energy shell averaging, where probabilities within each energy interval $\mathcal{M}_{\lambda, \Delta} = (\lambda - \Delta/2, \lambda + \Delta/2)$ are summed to form the binned probability $P(\mathcal{M}_{\lambda, \Delta}) = \sum_{\lambda_m \in \mathcal{M}_{\lambda, \Delta}} p_m^{\mu i}$. A Lorentzian fitting procedure applied to this binned distribution determines the characteristic parameters $\chi_{\mu i}$ and $\Delta_{\mu i}$. Figure fig. 1 demonstrates this methodology through representative calculations for two arbitrarily selected eigenstates, with insets showing good agreement between numerical results and Lorentzian fits. By fitting the distribution in eq. (33) for all states $\phi_{\mu i}$, we obtain the parameter evolution shown in fig. 3. Linear regression reveals:

$$\begin{aligned}\Delta_{\mu 1} &\approx -0.002\epsilon_\mu - 0.555 \\ \Delta_{\mu 2} &\approx -0.002\epsilon_\mu + 0.553.\end{aligned}\quad (40)$$

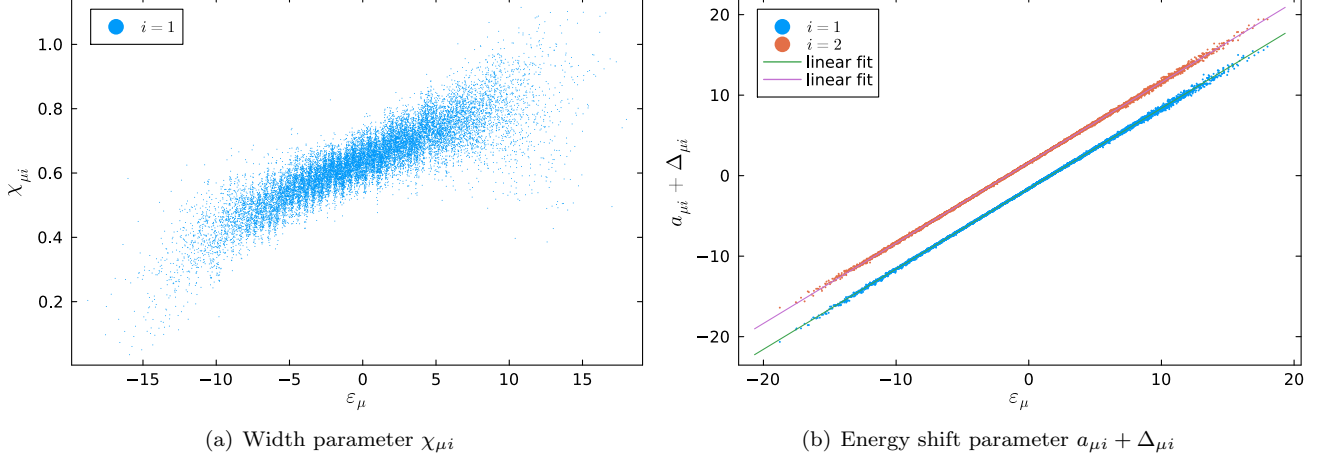


FIG. 3. Parameter evolution for $i = 1$. (a) Lorentzian width $\chi_{\mu i}$ versus bath energy ϵ_{μ} . (b) Linear regression of shifted energies yields $a_{\mu 1} + \Delta_{\mu 1} = 0.998\epsilon_{\mu} - 1.610$ and $a_{\mu 2} + \Delta_{\mu 2} = 0.998\epsilon_{\mu} + 1.608$, confirming energy-dependent shifts.

The self-consistency equations (36) and (37) are numerically verified in fig. 4. The remarkable agreement between direct parameter extraction and self-consistent solutions confirms our theoretical predictions.

To further analyze the interaction-driven broadening $\chi_{\mu i}$, we refer to eq. (13) and assume that we can replace $|V_{\mu i, \nu j}|^2$ with a smooth function $e^{-S(\epsilon_{\nu})} f_{i,j}^2(\epsilon_{\mu}, \delta)$, where $\delta = \epsilon_{\mu} - \epsilon_{\nu}$. In this way, the self-consistent equation (36) becomes

$$\chi_{\mu i} = \sum_j \int d\delta f_{i,j}^2(\epsilon_{\mu}, \delta) \frac{\chi_{\nu j}}{(\lambda - a_{\nu j} - \Delta_{\nu j})^2 + \chi_{\nu j}^2}. \quad (41)$$

The numerical characterization in fig. 2 reveals square-wave-like coupling profiles, assuming that their energy range is roughly $\mathcal{M}_{\epsilon_{\mu}, \Delta_I}$. This motivates the separation:

$$\chi_{\mu i} \approx \sum_j \mathcal{V}_{\mu i, j} \mathbb{E} \left(\frac{\chi_{\nu j}}{(\lambda - a_{\nu j} - \Delta_{\nu j})^2 + \chi_{\nu j}^2} \right), \quad (42)$$

where $\mathcal{V}_{\mu i, j} = \sum_{\nu} |V_{\mu i, \nu j}|^2$ and $\mathbb{E} = \frac{1}{\Delta_I} \int_{\epsilon_{\mu} + \Delta_I/2}^{\epsilon_{\mu} - \Delta_I/2} d\epsilon_{\nu}$ represents summing and averaging over energy shells $\mathcal{M}_{\epsilon_{\mu}, \Delta_I}$. The dominant cross-channel coupling $\mathcal{V}_{\mu 1, 2} \approx 1.982$ overwhelms the diagonal terms $\mathcal{V}_{\mu i, i} \approx 0.018$, indicating that the contribution of the diagonal term can be approximately neglected.

The self-consistent equation (42) contains numerous $\chi_{\mu i}$ and $\Delta_{\mu i}$, making it still a complex equation. Below we make the roughest estimate of $\chi_{\mu i}$ and $\Delta_{\mu i}$, coarse-grain them into simpler parameters and give the corresponding self-consistent equation. Assume that “the appropriate λ ” assumed previously in eq. (35) also has linear energy dependence

$$\lambda(\mu, i) = a_{\mu i} + \Delta_{\mu i} - \eta_i \quad (43)$$

Combining it with the fitting results (40) and the definition of $a_{\mu i}$, we get

$$\lambda(\mu, 1) - a_{\nu 2} - \Delta_{\nu 2} \approx \delta - \eta_1, \quad (44)$$

where $\delta = \epsilon_{\mu} - \epsilon_{\nu}$. According to fig. 3(a), $\chi_{\nu i}$ consists of a linear function about ϵ_{ν} plus some fluctuations. Here we approximately take it as the central value $\bar{\chi}_{\mu i} := \sum_{\epsilon_{\nu} \in \mathcal{M}_{\epsilon_{\mu}, \Delta}} \chi_{\nu i} / d\mathcal{M}$. According to fig. 4(b), the average of $\Delta_{\mu i} - V_{\mu i}$ is very close to a fixed value that does not change with ϵ_{μ} , let it be Δ_i . Based on these coarse-graining, ignoring the difference of $\bar{\chi}_{\mu i}$ under different i and the negligible $V_{\mu i}$, the self-consistent equation can be simplified to

$$\begin{aligned} \bar{\chi}_{\mu} &= \mathcal{V}_{\mu 1, 2} \mathbb{E} \left(\frac{\bar{\chi}_{\mu}}{(\delta - \eta_2)^2 + \bar{\chi}_{\mu}^2} \right), \\ \Delta_1 &= \mathcal{V}_{\mu 1, 2} \mathbb{E} \left(\frac{\delta - \eta_2}{(\delta - \eta_2)^2 + \bar{\chi}_{\mu}^2} \right). \end{aligned} \quad (45)$$

Assuming $\Delta_I = 2\alpha\bar{\chi}_{\mu}$ and $\eta_i = (-1)^{i-1}\beta\bar{\chi}_{\mu}$, then

$$\begin{aligned} \mathbb{E} \left(\frac{\bar{\chi}_{\mu}}{(\delta - \eta_2)^2 + \bar{\chi}_{\mu}^2} \right) &= \frac{\arctan(\alpha - \beta) + \arctan(\alpha + \beta)}{2\alpha\bar{\chi}_{\mu}}, \\ \mathbb{E} \left(\frac{\delta - \eta_2}{(\delta - \eta_2)^2 + \bar{\chi}_{\mu}^2} \right) &= \ln \left(\frac{1 + (\alpha - \beta)^2}{1 + (\alpha + \beta)^2} \right) / (4\alpha\bar{\chi}_{\mu}). \end{aligned} \quad (46)$$

Substituting it into eq. (45), we can get two equations about the three parameters $\bar{\chi}$, Δ_1 and η . As long as we know one of them, we can estimate the other two. According to figs. 2 and 4, consider the parameter average around $\epsilon_{\mu} = 0.583$. Numerical solutions with $\Delta_I = 4.216 + 2.985 \approx 7.2$, $\eta_i = (-1)^{i-1}2.63$, and $\mathcal{V}_{\mu 1, 2} \approx 1.982$ yield $\bar{\chi} \approx 0.67$ and $\Delta_2 = -\Delta_1 \approx 0.46$, which is roughly consistent with the fitting results in fig. 4. In the absence of prior knowledge about η_i , we assume it lies within the range from $\Delta_I/2$ (half width at half maximum of F^2) to 2.4 (half width at 99% maximum of F^2). This yields the parameter bounds $\bar{\chi} \in (0.42, 0.69)$

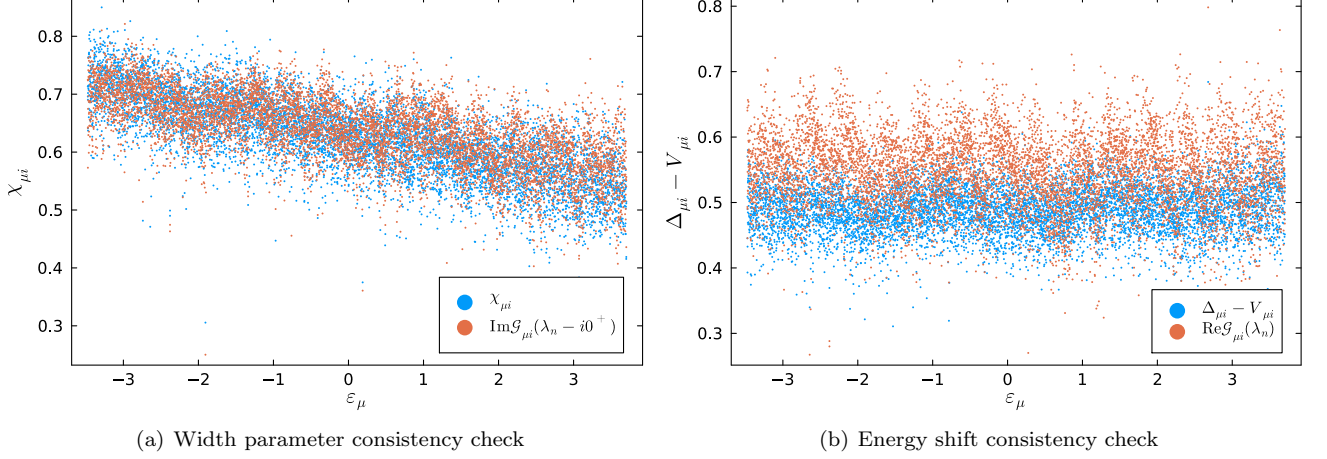


FIG. 4. Self-consistency validation for $i = 2$. (a) Orange: Directly fitted $\chi_{\mu i}$; Blue: Reconstructed values via eqs. (36) and (43). (b) Orange: Extracted $\Delta_{\mu i} - V_{\mu i}$; Blue: Calculated values using eqs. (37) and (43). In both (a) and (b), we used $\eta_i = (-1)^{i-1}2.63$.

and $-\Delta_1 \in (0.41, 0.65)$, as derived through our self-consistent analysis.

Finally, we compute the entropy production using the binomial approximation for density of states [15]:

$$e^{S(\lambda)} = \frac{\kappa N!}{(N/2 - \kappa\lambda)!(N/2 + \kappa\lambda)!}, \quad (47)$$

where $\kappa = \frac{1}{2}(g^2 + h^2 + 1)^{-1/2} \approx 0.344$. Under Gaussian approximation for binomial distributions:

$$e^{S(\lambda)} \approx 2^N \times G(\lambda; \sqrt{N}/(2\kappa)). \quad (48)$$

Combining it with eq. (38), we get

$$S(p^{\mu i}) \approx N \ln(2) - 2\kappa^2(a_{\mu i} + \Delta_{\mu i})^2/N + \ln(4\pi\chi_{\mu i}) - \ln[\pi N/(2\kappa^2)]/2. \quad (49)$$

As shown in fig. 5, the observational entropy aligns well with theoretical estimates using eq. (38), while von Neumann entropy reveals residual fluctuations.

V. OSCILLATIONS AROUND STEADY STATE

Steady state does not mean that the system-environment is always in this state, but oscillates around this state. For any bounded observable A , the temporal fluctuation amplitude is quantified by:

$$(\Delta\omega)_A^2 := \lim_{t \rightarrow \infty} \frac{1}{t} \int_0^t d\tau \{ \text{Tr}[A\rho(\tau) - A\omega] \}^2. \quad (50)$$

Following [10, 16], this fluctuation amplitude is upper bounded by the entanglement entropy (Rényi-2 entropy) of the steady state ω :

$$(\Delta\omega)_A^2 \leq \|A\|^2 e^{-S_2(\omega)}, \quad (51)$$

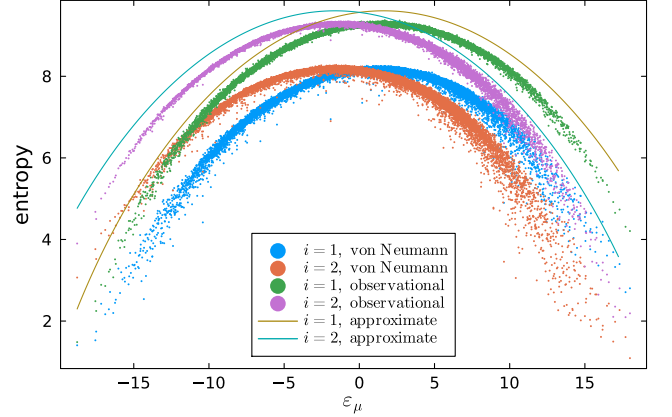


FIG. 5. Entropy comparison for different initial states μi . Observational entropy (energy shell positive operator-valued measure with $\Delta = 0.5$) closely matches theoretical estimates from eq. (49), using linear fits in fig. 3 (or equivalently eq. (40)) and averaged $\bar{\chi} = \sum_{\mu i} \chi_{\mu i}/2^N \approx 0.632$. Von Neumann entropy shows reduced values due to quantum fluctuations.

where S_α denotes the Rényi entropy:

$$S_\alpha(\rho) = \frac{1}{1-\alpha} \ln[\text{Tr}(\rho^\alpha)]. \quad (52)$$

For properties of entanglement entropy in specific systems, see [17].

Now we analyze the entanglement entropy corresponding to the Lorentzian ansatz (33). Substituting eq. (2) into the definition of entanglement entropy, and using the

smoothed distribution $p^{\mu i}(\lambda)$ like eq. (38), we get

$$\begin{aligned} S_2(\omega) &= -\ln\left[\sum_n (p_n^{\mu i})^2\right] \rightarrow S_2(p^{\mu i}) \\ &= -\ln\left\{\int d\lambda \frac{1}{e^{S(\lambda)}} \frac{1}{\pi^2} \frac{\chi_{\mu i}^2}{[(\lambda - a_{\mu i} - \Delta_{\mu i})^2 + \chi_{\mu i}^2]^2}\right\} \\ &\approx -\ln\left\{\int d\lambda \frac{1}{\pi^2} \frac{\chi_{\mu i}^2}{[(\lambda - a_{\mu i} - \Delta_{\mu i})^2 + \chi_{\mu i}^2]^2}\right\} \\ &\quad -\ln\left(\frac{1}{e^{S(a_{\mu i} + \Delta_{\mu i})}}\right) = S(a_{\mu i} + \Delta_{\mu i}) + \ln(2\pi\chi_{\mu i}), \end{aligned} \quad (53)$$

which is marginally smaller than the entropy (49). For large N in our nonintegrable model, the steady-state entanglement entropy grows linearly with N , causing the upper bound in eq. (51) to decay exponentially. This implies that post thermalization, the system executes negligible oscillations about the steady state. Consequently, the steady-state entropy effectively characterizes the system's thermodynamic behavior.

VI. ENHANCED ANSATZ FORMS AND ADDITIONAL CONSTRAINTS

In our preceding analysis, we implemented a minimal two-parameter Lorentzian ansatz. While this formulation demonstrates reasonable agreement with numerical results (Fig. 1(b)), its precision proves insufficient for more precise quantitative analysis. This limitation manifests through residual discrepancies in self-consistent equation verification (Fig. 4). Nevertheless, this two-parameter model remains adequate for primary investigations. To achieve enhanced accuracy, we propose several generalized formulations incorporating supplementary parameters for improved characterization of the $p^{\mu i}(\lambda)$ distribution.

Three critical features govern the $p^{\mu i}(\lambda)$ distribution: energy shift characteristics, spectral broadening, and tail behavior. Our initial ansatz (eq. (33)) assumes constant energy shifts and widths (eq. (35)) with Lorentzian tail profiles. We first consider tail modification through Voigt profile integration:

$$p^{\mu i}(\lambda) = \frac{1}{e^{S(\lambda)}} V(\lambda - a_{\mu i} - \Delta_{\mu i}; \sigma_{\mu i}, \chi_{\mu i}), \quad (54)$$

where the Voigt profile emerges from the convolution of Gaussian $G(x; \sigma) = e^{-x^2/(2\sigma^2)}/(\sqrt{2\pi}\sigma)$ and Lorentzian distributions:

$$V(x; \sigma, \chi) = \int dx' G(x'; \sigma) \frac{1}{\pi} \text{Im} \left(\frac{1}{x - x' - i\chi} \right). \quad (55)$$

This generalized ansatz introduces an additional broadening parameter $\sigma_{\mu i}$, recovering the original Lorentzian form when $\sigma_{\mu i} = 0$.

The introduction of supplementary parameters necessitates enhanced constraint analysis. A critical constraint emerges from subsystem probability summation:

$$p_n^i := \sum_{\mu} p_n^{\mu i} = \sum_{\mu} |\langle \psi_n | \phi_{\mu i} \rangle|^2 = \langle \phi_i^S | \rho_n^S | \phi_i^S \rangle, \quad (56)$$

where $\rho_n^S = \text{Tr}_B(|\psi_n\rangle\langle\psi_n|)$ represents the reduced density matrix. The bath energy density of states approximates as [15]:

$$e^{S'(\epsilon)} = \frac{\kappa'(N-1)!}{((N-1)/2 - \kappa'\epsilon)!((N-1)/2 + \kappa'\epsilon)!}, \quad (57)$$

with $\kappa' = \frac{1}{2}[g^2 + h^2 + 1 - 1/(N-1)]^{-1/2} \approx 0.350$. Substituting eq. (33) into eq. (56) yields:

$$p_n^i = \int d\epsilon_{\mu} e^{S'(\epsilon) - S(\lambda_n)} V(\lambda - a_{\mu i} - \Delta_{\mu i}; \sigma_{\mu i}, \chi_{\mu i}). \quad (58)$$

Under Gaussian approximation for binomial distributions (48) and assuming $\chi_{\mu i}$, $\sigma_{\mu i}$, and $\Delta_{\mu i}$ remain constant across ϵ_{μ} variations, convolution theorem gives:

$$\begin{aligned} p_n^i &= 1/[2G(\lambda_n; \sqrt{N}/(2\kappa))] \\ &\quad \times V(\lambda_n - E_i - \Delta_i; \sqrt{(N-1)/(2\kappa')^2 + \sigma_i^2}, \chi_i). \end{aligned} \quad (59)$$

The trace condition $\sum_i p_n^i = \text{Tr} \rho_n^S = 1$ constrains χ_i , σ_i , and Δ_i relationships. Subsequent ETH considerations suggest local thermalization:

$$\rho_n^S \sim \rho^{\text{can}} = \sum_i e^{-\beta_n(E_i + \Delta_i)} \Pi_{\phi_i}^S / Z_n, \quad (60)$$

where $\beta_n = \partial_{\lambda} S(\lambda_n)$. This relationship serves dual purposes: constraining parameter space and validating ETH compliance.

We further extend width characterization through functional modification $\chi_{\mu i} \rightarrow \chi_{\mu i}(\lambda) = \chi_{\mu i} + \theta_{\mu i} \lambda^2$, preserving normalization:

$$p^{\mu i}(\lambda) = \frac{1}{e^{S(\lambda)}} \frac{1}{\pi Z_{\mu i}} \frac{\chi_{\mu i} + \theta_{\mu i} \lambda^2}{(\lambda - a_{\mu i} - \Delta_{\mu i})^2 + (\chi_{\mu i} + \theta_{\mu i} \lambda^2)^2}, \quad (61)$$

with normalization factor:

$$Z_{\mu i} = \text{Re} \left[\frac{2}{\sqrt{1 + 4\theta_{\mu i}(\chi_{\mu i} + i\Delta_{\mu i})}} \right] - \mathbf{1}_{\{0\}}(\theta_{\mu i}), \quad (62)$$

where $\mathbf{1}_A(x)$ is indicator function. For refined precision, we propose a quadratic extension:

$$p^{\mu i}(\lambda) = \frac{(\chi_{\mu i} + v_{\mu i} \lambda + \theta_{\mu i} \lambda^2)/(e^{S(\lambda)} \pi Z'_{\mu i})}{(\lambda - a_{\mu i} - \Delta_{\mu i})^2 + (\chi_{\mu i} + v_{\mu i} \lambda + \theta_{\mu i} \lambda^2)^2}, \quad (63)$$

where $\theta_{\mu i} \neq 0$ and normalization:

$$Z'_{\mu i} = \text{Re} \left[\frac{2}{\sqrt{1 + 4\theta_{\mu i}(\chi_{\mu i} + i\Delta_{\mu i}) - v_{\mu i}(v_{\mu i} - 2i)}} \right]. \quad (64)$$

Energy shift generalization $\Delta_{\mu i} \rightarrow \Delta_{\mu i}(\lambda)$ follows similar procedures.

Ultimate refinement incorporates composite profiles:

$$p^{\mu i}(\lambda) = \frac{1}{e^{S(\lambda)}} \int dx' G(x'; \sigma) \frac{1}{\pi Z_{\mu i}^{\Delta, \chi}} \times \text{Im} \left(\frac{1}{\lambda - a_{\mu i} - \Delta_{\mu i}(\lambda) - x' - i\chi_{\mu i}(\lambda)} \right), \quad (65)$$

where the normalization factor $Z_{\mu i}^{\Delta, \chi}$ is determined via pole expansion to satisfy:

$$\int d\lambda \frac{1}{\pi Z_{\mu i}^{\Delta, \chi}} \text{Im} \left(\frac{1}{\lambda - a_{\mu i} - \Delta_{\mu i}(\lambda) - x' - i\chi_{\mu i}(\lambda)} \right) = 1. \quad (66)$$

Detailed investigation of these advanced formulations exceeds our current scope and will be addressed in subsequent studies.

VII. CONCLUSION AND DISCUSSION

We have established a universal mechanism for steady-state entropy production in isolated quantum systems obeying the ETH, demonstrating that generic interaction-induced eigenstate mixing leads to intrinsic entropy growth independent of specific coupling details. Through analytical arguments supported by numerical simulations of nonintegrable spin chains, we identified two universal entropy-generation pathways: (1) energy-broadening effects governed by interaction bandwidth, and (2) temporal averaging over exponentially small energy gaps. Our resolvent-based framework resolves longstanding debates about the interplay between interaction strength and entropy scaling by revealing logarithmic dependence on Lorentzian broadening parameters, $S(\omega) \approx S(a_{\mu i} + \Delta_{\mu i}) + \ln(4\pi\chi_{\mu i})$, directly derived from ETH-governed matrix element statistics.

Key innovations include the derivation of self-consistent equations for probability distributions $p_n^{\mu i}$ through resolvent analysis, bypassing restrictive random-matrix assumptions. Numerical validation using an Ising spin chain with transverse/longitudinal fields confirms the predicted Lorentzian energy broadening (fig. 1) and parameter evolution (figs. 3 and 4). The observed linear scaling of energy shifts $\Delta_{\mu i}$ (eq. (40)) and width parameters $\chi_{\mu i}$ with bath energy underscores the universality of our framework. Notably, the dominance of cross-channel couplings ($\mathcal{V}_{\mu 1,2} \gg \mathcal{V}_{\mu i,i}$) reveals that off-diagonal ETH correlations drive entropy production, while diagonal terms contribute negligibly.

Our estimated entropy, calculated using a smoothed distribution analogous to observational entropy that neglects probability fluctuations within energy shells, yields results closer to observational entropy as illustrated in fig. 5. To enable direct comparison with the von Neumann entropy of the original distribution, a systematic incorporation of the probability fluctuations within the

energy shell would be required. In theory, these can be obtained by further analyzing the variance and higher-order moments of the probability distribution of each energy shell. Since the self-consistent equation eq. (27) is not smoothly approximated, one can add higher-order terms on the basis of the assumed eq. (33) to study the variance and higher-order moments of the probability distribution, thereby obtaining a more accurate entropy estimate.

Practically, the derived logarithmic entropy scaling provides a predictive tool for quantum technologies requiring entropy control. The identified universal features, particularly the decoupling of entropy growth from microscopic interaction details, suggest broad applicability across condensed matter and cold-atom platforms. For instance, this principle enables: Analysis of non-equilibrium dissipation in high-temperature superconducting phase transitions by controlling entropy generation via electron-electron interactions; Enhancement of energy conversion efficiency in cold-atom thermal engines through optimized interaction-driven entropy production; Verification of non-equilibrium physics theories via entropy dynamics in tunable many-body systems. Future extensions should address (i) variance analysis of $p_n^{\mu i}$ distributions beyond Lorentzian ansatz, (ii) multi-scale entanglement dynamics during prethermalization, and (iii) experimental protocols for measuring energy-shell resolved observational entropy. These advances will further unify quantum thermodynamics with practical entropy engineering in complex systems.

Finally, we note that our analytical framework fundamentally relies on the ETH assumption, which allows off-diagonal matrix elements to behave as random variables. Under ETH, complex cross-correlated interaction terms average out, enabling a closed set of self-consistent equations for the projected resolvent $\mathcal{R}_{\mu i}(z)$ and entropy growth. In some special cases, when ETH is violated, such as in strictly integrable or many-body-localized (MBL) systems, these simplifications no longer apply. Integrable models possess extensive conserved quantities and admit explicit eigenstate solutions (e.g. via Bethe ansatz or free-fermion methods), so that the entropy of decohered state can be determined directly without invoking our ETH-based mechanism. By contrast, MBL systems strongly violate ETH and exhibit anomalously slow thermalization; the generic entropy scaling predicted here (e.g. logarithmic growth) is not expected to hold, and the fate of observational entropy in such phases remains an open question. Characterizing entropy production beyond the ETH paradigm thus requires new theoretical tools and remains an important subject for future research.

ACKNOWLEDGMENTS

This work is supported by the National Natural Science Foundation of China under Grant No. 12305035

-
- [1] J. M. Deutsch, Quantum statistical mechanics in a closed system, *Phys. Rev. A* **43**, 2046 (1991).
 - [2] M. Srednicki, Chaos and quantum thermalization, *Phys. Rev. E* **50**, 888 (1994).
 - [3] C. Gogolin and J. Eisert, Equilibration, thermalisation, and the emergence of statistical mechanics in closed quantum systems, *Rep. Prog. Phys.* **79**, 056001 (2016).
 - [4] L. D'Alessio, Y. Kafri, A. Polkovnikov, M. Rigol, From quantum chaos and eigenstate thermalization to statistical mechanics and thermodynamics, *Advances in Physics*, **65** (2016) 239-362.
 - [5] D. Šafránek, J.M. Deutsch, A. Aguirre, Quantum coarse-grained entropy and thermodynamics, *Physical Review A*, **99** (2019) 010101.
 - [6] D. Šafránek, A. Aguirre, J. Schindler, J.M. Deutsch, A Brief Introduction to Observational Entropy, *Foundations of Physics*, **51** (2021) 101.
 - [7] T. Nagasawa, K. Kato, E. Wakakuwa, F. Buscemi, Generic increase of observational entropy in isolated systems, *Physical Review Research*, **6** (2024) 043327.
 - [8] P. Figueroa-Romero, K. Modi, F.A. Pollock, Equilibration on average in quantum processes with finite temporal resolution, *Physical Review E*, **102** (2020) 032144.
 - [9] E. Iyoda, K. Kaneko, T. Sagawa, Eigenstate fluctuation theorem in the short- and long-time regimes, *Physical Review E*, **105** (2022) 044106.
 - [10] A.J. Short, Equilibration of quantum systems and subsystems, *New Journal of Physics*, **13** (2011) 053009.
 - [11] M. Ippoliti, W.W. Ho, Solvable model of deep thermalization with distinct design times, *Quantum*, **6** (2022) 886.
 - [12] D.K. Mark, F. Surace, A. Elben, A.L. Shaw, J. Choi, G. Refael, M. Endres, S. Choi, Maximum Entropy Principle in Deep Thermalization and in Hilbert-Space Ergodicity, *Physical Review X*, **14** (2024) 041051.
 - [13] T. Helbig, T. Hofmann, R. Thomale, M. Greiter, Theory of Eigenstate Thermalisation, *arXiv preprint arXiv:2406.01448*, DOI (2024).
 - [14] L. Foini, J. Kurchan, Eigenstate thermalization hypothesis and out of time order correlators, *Physical Review E*, **99** (2019) 042139.
 - [15] A. Dymarsky, N. Lashkari, H. Liu, Subsystem eigenstate thermalization hypothesis, *Physical Review E*, **97** (2018) 012140.
 - [16] H. Wilming, M. Goihl, I. Roth, J. Eisert, Entanglement-Ergodic Quantum Systems Equilibrate Exponentially Well, *Physical Review Letters*, **123** (2019) 200604.
 - [17] L.-K. Lim, C. Lou, C. Tian, Mesoscopic fluctuations in entanglement dynamics, *Nature Communications*, **15** (2024) 1775.